ODSIM: An Object-Distance Simulation method for Conditioning Complex Natural Structures [1]

Vincent Henrion [2][3][4] Guillaume Caumon [3][5]

Nicolas Cherpeau [3][6]

December 22, 2011

Submitted to Mathematical Geosciences

[1]Received ; accepted .

[2]Corresponding author

[3]Nancy-Université, Centre de Recherches Pétrographiques et Géochimiques, École Nationale Supérieure de Géologie, Rue du doyen Marcel Roubault, 54501 Vandoeuvre-lès-Nancy, France

[4]e-mail: henrion@gocad.org

[5]e-mail: Guillaume.Caumon@ensg.inpl-nancy.fr

[6]e-mail: cherpeau@gocad.org

Abstract

Stochastic simulation of categorical objects is traditionally achieved either with object-based or pixel-based methods. Whereas object-based modeling provides realistic results but raises data conditioning problems, pixel-based modeling provides exact data conditioning but may lose some features of the simulated objects such as connectivity. We suggest a hybrid dual-scale approach to combine both shape realism and strict data conditioning. The procedure combines the distance transform to a skeleton object representing coarse-scale structures, plus a classical pixel-based random field and threshold representing fine-scale features. This object-distance simulation method (ODSIM), uses a perturbed distance to objects, and is particularly appropriate for modeling structures related to faults or fractures such as karsts, late dolomitized rocks and mineralized veins. We demonstrate this method to simulate dolomite geometry and discuss strategies to apply this method more generally to simulate binary shapes.

KEYWORDS: Geostatistics, Gibbs sampler, Gaussian stochastic process, Object-based simulation, implicit representation, Euclidean distance transform

1 Introduction

Stochastic simulation is commonly used in various geoscience fields for modeling subsurface heterogeneity. Stochastic simulations aim at generating

multiple (equiprobable) numerical models, termed *realizations*, which reproduce the heterogeneity expected in the reality while honoring available data (Haldorsen and Damsleth, 1990). The heterogeneity model being reproduced is typically described either by a variogram (e.g. Deutsch and Journel, 1998; Goovaerts, 1997; Chilès and Delfiner, 1999), a training image (e.g. Strebelle, 2002; Arpat and Caers, 2007) or a parametric object model (e.g. Deutsch and Wang, 1996; Holden et al., 1998; Viseur, 2004; Allard, Froideveaux and Biver, 2006). These methods do not explicitly make assumptions or try to reproduce geological processes, for data conditioning would then make stochastic simulation impractical. However, subsurface petrophysical properties are generally controlled by genetic constraints (*e.g.*, crystallization, sedimentary processes), followed by secondary transformations (*e.g.* structural events, diagenesis, hydrothermal alteration). While the stochastic simulation of sedimentary rocks has been widely studied, heterogeneities due to later processes have received less attention (Labourdette et al., 2007; Boisvert et al., 2008), except for fractures (e.g. Gringarten, 1998; Srivastava, Frykman and Jensen, 2004). The main motivation of this work is therefore to propose a general method to account for late underground processes affecting rock features. Therefore, we suggest modeling the geometry of geological bodies which result from geological processes occurring in relation to pre-existing objects. This is the case for instance in hydrothermal-related ore deposits, caves and paleocaves, dolomitized formations. For this, we propose combining an object-based representation of pre-existing rock features and a stochastically

perturbed Euclidean distance transform. After providing more details about this object-distance Simulation method (ODSIM, Section 2), we present a typical application to a hydrothermal dolomite formation (Section 3.1). The ODSIM method is also applicable to other contexts, as demonstrated in Section 2.4 by the generation of a micro-scale porous medium and of meandering channels in Section 3.2.

2 The ODSIM Approach

2.1 Approach Overview

Figure 1 illustrates on a simple example the principles of the ODSIM methodology. The simulation procedure first calls for one or multiple object models considered as the skeleton of the geological body to be simulated (Section 2.2). The idea of using skeleton object as been also introduced by Yin et al. (2009) to reconstruct 2D channels from channel centerlines and multiple point statistics. The skeleton in Figure 1 is a single line embedded in a 3D Cartesian grid. The ODSIM method then computes the Euclidean distance transform to this skeleton, resulting in a 3D distance field (Section 2.3). The latter can be viewed as a potential field, i.e., the probability to be in the geological body decreases when moving away from the skeleton. A spatially correlated random field (threshold) is then stochastically simulated to perturb the distance field. The simulated body is obtained by thresholding the difference of the

distance and the random field. The random field is simulated imposing various spatial parameters (probability density function –pdf– and variogram) to control the extension and sinuosity of the geological bodies (Section 2.4). Despite the simplicity of this approach, it can be used to generate very different object shapes by appropriately choosing the skeleton object and random field features. Conditioning to well data is obtained by iterative Gibbs sampling with inequality constraints in order to preserve both the spatial structure and histogram of the random field (Section 2.5).

[Figure 1 about here.]

2.2 Definition of the skeleton object

Applying ODSIM relies on a first stage of generating a skeleton object consistent with the target spatial phenomenon and representing first-order spatial features. For some modeling problems, the "nature" of the skeleton object may be very intuitive. For instance, post-depositional structures as karst conduits, mineralization veins or dolomitization usually originate along fractures or faults which act as preferential flow paths and hence favor rock transformations. In this case, the skeleton object may simply consist of 3D polygons or free-form surfaces. To give just a few more examples, the skeleton object for simulating 2D channels could consist of sinusoidal center lines, or a set of 3D points or sphere to generate pore-scale models. Once the characteristics of the skeleton have been determined, various approaches may be examined

to generate effectively the skeleton object. It may be defined in a deterministic fashion, or obtained from object-based simulation. For example, regarding the simulation of fracture-related zones, fracture or fault objects may originate from geological mapping based on aerial photograph, outcrop, or subsurface interpretation from seismic images. When poorly constrained by observations, fracture networks may also be generated using object-based simulation. Object-based methods may simulate diverse types of shapes to account for prior geological knowledge. Moreover, locally varying density and orientation may be used to constrain respectively the local number of objects and their orientation. Attraction or repulsion rules may also be implemented in order to account for interaction between objects. To ensure proper conditioning of the geological bodies to observation data, spatial trends can be used during object-based skeleton simulation so that approximate conditioning is achieved (Stoyan, Kendall and Mecke, 1995; Lantuéjoul, 2002). Also, simulated skeleton objects may be filtered before applying further steps of ODSIM. For instance graphs of connectivity may be used to select only connected paths of skeleton objects. This selection step can be used to filter object-based simulation results and mimic selective processes such as dissolution of carbonate rocks around favorable fractures when modeling cave geometry (Henrion, Pellerin and Caumon, 2008). It may also be used to rapidly account for dynamic data, as proposed by Renard and Caers (2008) in the context of pixel-based simulation.

For a new modeling problem, several questions come up to apply ODSIM:

can the target geological body be reduced to a skeleton object? Can realistic geometries be reproduced when randomly truncating the skeleton related distance field? What is the sensitivity of the final results to the skeleton object? In following sections we describe strategies to construct skeleton objects for simulating different problems such as dolomite body, micro-porous medium and channels. In other applications, these questions should be addressed on a case-by-case basis.

2.3 Euclidean distance field

Reproducing geometry of geological features around the skeleton relies on the knowledge of the distance to the object. Let S denote the set of objects constituting the skeleton object embedded in a grid G . A Euclidean distance field associated to each point $\mathbf{p} = [p_x p_y p_z]^T$ of G is the Euclidean distance from that point to the closest point $\mathbf{q} = [q_x q_y q_z]^T$ belonging to any object of S:

$$D(\mathbf{p}) = \min\{dist_E(\mathbf{p}, \mathbf{q}),\ \mathbf{p} \in G,\ \mathbf{q} \in S\} \tag{1}$$

where the function $dist_E$ is the distance between $\mathbf{p}$ and $\mathbf{q}$ given a Euclidean metric:

$$dist_E(\mathbf{p}, \mathbf{q}) = \sqrt{(p_x - q_x)^2 + (p_y - q_y)^2 + (p_z - q_z)^2} \tag{2}$$

A review of techniques to compute 3D distance field is proposed by Jones, Baerentzen and Srame (2006). In this work, we compute the 3D Euclidean distance transform on a Cartesian grid with the algorithm introduced by Saito and Toriwaki (1994) and implemented by Ledez (2003). This efficient, linear complexity algorithm simply rasterizes the skeleton objects, then computes the distance field by traversing the grid six times, twice along each axis.

After this step, the explicit representation of the skeleton object is defined implicitly as the iso-value 0 (denoted S_0) of the distance field D on grid G:

$$S_0 = \mathbf{p} \in G |\ D(\mathbf{p}) = 0 \tag{3}$$

This distance field can also be used as constraint for defining geological features. Typically, the probability for a point to be in a geological body decreases when moving away from the skeleton object and becomes null beyond a given distance threshold. Therefore, an iso-value $\varphi \neq 0$ of the distance field D may be used to extract the coarse-scale envelope of the geological bodies to generate. These objects are identified by a binary categorical property I_B defined for each point $\mathbf{p}$ of grid G:

$$I_B(\mathbf{p}) = \begin{cases} 1 & \text{if } D(\mathbf{p}) \leq \varphi \\ 0 & \text{if not} \end{cases} \tag{4}$$

Note that the computation of the distance field is not restricted to an Euclidean metric. We show for instance in section 2.5 how anisotropic distances

can be used to further introduce trends into the generated models.

2.4 Stochastic perturbation of distance field

Using a constant distance threshold φ to extract geological object generates extremely smooth objects, and does not easily allow for conditioning to observation data. More realistic geometries of geological bodies may be obtained by simulating a spatially correlated random field $\varphi(\mathbf{p})$ acting as a distance threshold in the grid G. Therefore, Equation (4) is modified as follows to add fine-scale variability to the coarse-scale object:

$$I_B(\mathbf{p}) = \begin{cases} 1 & \text{if } D(\mathbf{p}) \leq \varphi(\mathbf{p}) \\ 0 & \text{if not} \end{cases} \tag{5}$$

The threshold $\varphi(\mathbf{p})$ may be generated using Sequential Gaussian Simulation (Deutsch and Journel, 1998), or other stochastic simulation methods (Emery and Lantuéjoul, 2006; Journel , 1994; Yao, 1998). The probability density function (pdf) of the simulated threshold values and its variogram model provide controls on the geometric features of the simulated geological bodies.

[Figure 2 about here.]

The definition of model parameters (e.g. facies proportion, object density, variogram, selection of a training image, etc.) is a key process for all geostatistical algorithms. Provided that the skeleton object is readily obtained, a user

applying ODSIM needs to define a distribution model and variogram model to inform random field simulations. The distribution model of threshold values controls the size of the features, while the parameters of the variogram model, principal ranges and principal directions, control respectively the sinuosity and the orientation of the final features around the skeleton (Figure 2). Hence, the choice of model parameters should consider the geometrical characteristics of the target spatial phenomenon. However, in most cases, neither the true feature geometry nor their spatial distribution can be observed or described with certainty at locations of relevance. Consequently, the application of geostatistical methods often requires a priori geological knowledge to define the extension, shapes and distribution of the target geological features. From expert knowledge, actual measurements on analog systems or physically-based models, there are two possible approaches to incorporate a priori geological knowledge when applying ODSIM : (a) well-log data and seismic survey may provide information about object distribution and geometry and then relate object parameters from prior geological knowledge to actual subsurface objects (Caers , 2005). This approach is not specific to ODSIM and is commonly applied for other geostatistical methods. (b) the second approach consists in directly inferring the model parameters from a training image that represent geometrical/geological features deemed representative of the target pattern (Strebelle, 2002; Journel , 2006). In that case, computation of the medial axis of the target features present in the training image provides insights about the skeleton object characteristics. Parame-

ters of the random field may also be obtained from the distance between the medial axis and object boundaries : the histogram and variogram of this distance provide the global statistics to be used for generating the threshold random field. This is illustrated in figure 3 where the medial axis of a reference pore-scale model has been computed to obtained the distribution and variogram model of the local width of pore phase. This statistics has then been used to generate the random threshold field and produce multiple realizations of porous medium all different in details but sharing the same statistics as the reference model.

[Figure 3 about here.]

2.5 Conditioning to well data

2.5.1 Hard data conditioning

Realizations honoring point observations are obtained when the simulated random threshold field is higher than or equal to (resp. lower than) the distance value where feature presence are observed (resp. absent). Stochastic simulation easily accounts for scalar values, so the main point of data conditioning is to find some possible scalar threshold value at each binary observation data point (Figure 4), hence to run a simulation under inequality constraints (Dubrule and Kostov, 1986). Let I_F denote a categorical variable indicating the presence ($I_B(\mathbf{p}) = 1$) or the absence ($I_B(\mathbf{p}) = 0$) of geological body, and $D(\mathbf{p})$ the distance value at data location $\mathbf{p}$. Then, the scalar

threshold $\varphi(\mathbf{p})$ to be considered during simulation is constrained by:

$$\varphi(\mathbf{p}) \in \begin{cases} [D(\mathbf{p}), max] & \text{if } I_B(\mathbf{p}) = 1 \\ [min, D(\mathbf{p})[& \text{if } I_B(\mathbf{p}) = 0 \end{cases} \tag{6}$$

[Figure 4 about here.]

This data transformation should honor the spatial covariance model to be used during threshold simulation. For this, we use the method introduced by Freulon and de Fouquet (1993) for conditioning a Gaussian random field with inequalities. It consists in an iterative algorithm based on the Gibbs sampler (Geman and Geman, 1984):

1. The data are transformed into threshold values verifying Equation (6) by Monte-Carlo sampling from the input threshold pdf. During this initialization stage, the spatial correlation is ignored since values are simulated independently one from another.

2. The initial threshold values are iteratively modified until the desired spatial correlation is reached. During an iteration step, each data location is visited in random order, and the current threshold is replaced by a value sampled from its conditional distribution estimated by simple kriging of neighboring data. A standardization procedure forces the threshold value to remain in the desired interval.

This method is known to be sometimes slow and convergence may be difficult to reach. Note however, that the transformation may be applied only once

and only on the observations whose number is generally far smaller than the number of grid cells to be simulated. We have run this transformation on a set of hundred wells sampled from a reference boolean model. Each wells is vertical and composed of 40 observations. For this case, convergence to the variogram model was obtained after approximately 25 iterations and in less time than one minute on a 2.8Ghz, 2GB RAM desktop PC. More details on the mathematics and convergence rate of the Gibbs sampler are given by Freulon and de Fouquet (1993). Once well data have been transformed into continuous values, the full-field simulation can be done by a direct method such as sequential Gaussian simulation or spectral simulation (Yao, 1998).

2.5.2 Soft data conditioning

In addition to hard data conditioning, the method allows for integrating soft constraints. For instance, spatial trend in object size or orientation may be accommodated in the random threshold field by specifying a locally variable mean. This is illustrated in Figure 5A where the threshold has been simulated with local mean increasing towards the right of the image. Note also that the distance field need not be Euclidean, but may account for anisotropy or locally variable metric tensor. In Figure 5B such anisotropic distance has been computed to induce different object sizes.

[Figure 5 about here.]

2.6 Postprocessing

As shown in Figure 6, regions disconnected from the main geological bodies may results from the ODSIM method. This especially occurs when the sinuosity of the simulated body is high, i.e., when the threshold field is simulated with short variogram range as compared to the distance field. Such disconnected features may be unrealistic with regard to the parent geological processes, for instance involving the propagation of a reactive front. As there are no easy direct way to avoid these features, we suggest to filter out of small isolated bodies deemed unrealistic. This can be performed using image processing techniques (Serra, 1988). Note however that this is done at the expense of the target proportion. A more complex cleaning routine could be used by iteratively removing disconnected component and branching or expanding others to keep the target proportion (Favilene et al. , 2009).

[Figure 6 about here.]

3 Examples

3.1 Simulating hydrothermal dolomites

The purpose of this example is to produce realistic images of dolomite bodies with plume-like geometry. Most dolomites are regarded as replacement of pre-existing limestone. Dolomitizing fluids migrate along faults and dif-

fuse laterally into adjacent limestone following fractures and more permeable strata (Davies and Smith, 2006, and references therein). We used a synthetic example consisting in a Cartesian grid of $150 \times 100 \times 60$ voxels and a vertical fault crossing the zone. Two different sets of horizontal planes were simulated by a marked Poisson point process (Stoyan, Kendall and Mecke, 1995). Together with the main fault, these planes constitute the initial skeleton object model (Fig. 7A). The corresponding distance field is shown in Figure 7B and random threshold in Figure 7C. Finally the truncation of the distance field with the random threshold given Eq.(5) generates binary images of dolomite bodies (Fig. 7D). The iso-surface of the dolomite bodies colored with depth values is displayed in Figure 7E. The latter illustrates the variety of shapes and sizes that can be generated with ODSIM while preserving the global connectivity of the simulated body.

[Figure 7 about here.]

3.2 Simulating channels

The purpose of this example is to improve the conditioning of hard data when simulating channels with object-based simulations. Indeed, it is well known that the conditioning of local data by random objects can be difficult with boolean object-based algorithms. In figure 8A, channels have been simulated using FluvSim (Deutsch and Wang, 1996) . Data which are not honored are highlighted by the red arrows. For each realization we extracted the medi-

als axis of channels to constitute the skeleton object (Fig.8b) and perform ODSIM in a similar way as described for porous models (Fig.3). Using the iterative Gibbs sampling described in Section 2.5, binary data are transformed into threshold values according to the target histogram (channels width) and variogram (channel sinuosity). Finally, channel realizations are obtained by truncating the distance field by the conditional threshold. As a result, we can see in Figure 8 modification of the channels where data were initially not honored. Note however that this procedure does not ensure exact conditioning. This comes from the incompatibility between the location of some data, the input channel configuration and the target histogram. Indeed, to ensure channel conditioning (resp. non channels conditioning) the distance between a point on the skeleton object and the data point must not exceed the minimal value (resp. the maximal value) of the threshold histogram. In the upper part of the channel realization (Fig. 8D) a channel observation has not been honored because the distance of this point to the closest point on the skeleton object is not in the histogram range. A solution to this problem would be to use some approximate conditioning of channels when running object-based simulation to force an object to be further or closer to an observation point than a given distance, i.e. relaxing their global conditioning to data. The benefit of such an approximate conditioning would be the performance of the simulated annealing/birth-death process which are reputably slow in the presence of dense data.

[Figure 8 about here.]

4 Conclusion

We have proposed a dual-scale geostatistical simulation method, whereby first-order features are represented by the distance to a discrete object model, and fine-scale features are modeled by a classical random field perturbing the distance field. This decoupling has several advantages. First, it can benefit from deterministic coarse-scale models or from object-based simulation method while relaxing their global conditioning to observation data. It can also incorporate connectivity information at the coarse-scale; this connectivity is preserved by the fine-scale perturbation. Truncation of the distance field by a random threshold then provides exact conditioning together with fine-scale details. The parameters of the method should be carefully adapted to the problem at hand; we have proposed strategies to set the parameters for modeling fault and fracture related heterogeneities as well as for porous models and channels. We believe this method could be extended to other modeling purpose and that it complements the set of available geostatistical methods to accurately represent the complexity of subsurface heterogeneity.

5 Acknowledgments

This research was performed in the frame of the Gocad research project. The companies and universities members of the Gocad consortium (`http://www.gocad.org`) are acknowledged for supporting this work.

References

Allard D, Froideveaux R, Biver P (2006) Conditional simulation of multi-type non stationary markov object models respecting specified proportions. Math Geol 38(8):959–986

Arpat GB, Caers JK (2007) Conditional simulation with patterns. Math Geol 39(2):177–203

Boisvert J, Leuangthong O, Ortiz J, Deutsch CV (2008) A methodology to construct training images for vein-type deposits. Comput Geosci 34(5):491–502

Caers J(2005) Petroleum Geostatistics. SPE Interdisciplinary Primer Series, Society of Petroleum Engineers, Richardson, TX, 96p.

Chilès JP, Delfiner P (1999) Geostatistics: Modeling Spatial Uncertainty. Series in Probability and Statistics, John Wiley and Sons, New York

Davies G, Smith L Jr (2006) Structurally controlled hydrothermal dolomite reservoir facies: an overview. AAPG Bull 90(11):1641–1690

Deutsch C, Journel A (1998) GSLIB: geostatistical software library and user's guide. Oxford University Press, New York

Deutsch CV (1998) Fortran programs for calculating connectivity of three-

dimensional numerical models and for ranking multiple realizations. Comput Geosci 24(1):69–76

Deutsch CV, Wang L (1996) Hierarchical object-based stochastic modeling of fluvial reservoirs. Math Geol 28(7):857–880

Dubrule O, Kostov C (1986) An interpolation method taking into account inequality constraints: I. Methodology Math Geol 18(1):33–51

Emery X, Lantuéjoul C (2006) TBSIM: A computer program for conditional simulation of three-dimensional Gaussian random fields via the turning bands method. Comput Geosci 32(10):1615–1628

Favilene O, Cabello P, Arbués P, Munoz JA, Cabrera L (2009) A geostatistical algorithm to reproduce lateral gradual facies transitions. Comput Geosci 35:1642-1651

Freulon X, de Fouquet C (1993) Conditioning a Gaussian model with inequalities in: Soares A (ed.) Geostatistics Tróia '92 volume 1 201–212 Kluwer Academic, Dordrecht

Geman S, Geman D (1984) Stochastic relaxation, gibbs distribution and the bayesian restoration of images. IEEE Trans Pattern Anal Mach Intell 6(6):721–741

Goovaerts P (1997) Geostatistics for natural resources evaluation Applied Geostatistics Oxford University Press, New York

Gringarten E (1998) FRACNET : Stochastic simulation of fractures in layered systems. Comput Geosci 24(8):729–736

Haldorsen HH, Damsleth E (1990) Stochastic modeling. J Pet Sci Technol 42:404–412

Henrion V, Pellerin J, Caumon G (2008) A stochastic methodology for 3D cave systems modeling in: Ortiz J, Emery X (eds.) Proceedings of the Eight International Geostatistics Congress volume 1 525–533 Gecamin ltd, Santiago

Holden L, Hauge R, Skare A, Skorstad A (1998) Modeling of fluvial reservoirs with object models. Math Geol 30(5):473–496

Jones M, Baerentzen J, Sramek M (2006) 3d distance fields: a survey of techniques and applications. IEEE Trans Visual Comput Graphics 12(4):581–599

Journel AG, (1994) Modeling Uncertainty: Some conceptual thoughts. in: Dimitrakopoulos R et al. Geostatistics for the next century, Kluwer, Dordrecht, Holland 30–43

Journel AG, (2006) The necessity of multiple-point prior model. Math Geol 38(5):591–610

Labourdette R, Lascu I, Mylroie J, Roth M (2007) Process-like modeling of flank-magin caves: from genesis to burial evolution. J Sediment Res 77(10):965–979

Lantuéjoul C (2002) Geostatistical Simulation : Models and Algorithms. Springer, Berlin, Germany

Ledez D (2003) Modélisation d'objets naturels par formulation implicite. Ph.D. thesis INPL Nancy, France

Lindquist W, Lee S, Coker D, Jones K, Spanne P (1996) Medial axis analysis of void structure in three-dimensional tomographic images of porous media. J Geophys Res [Solid Earth] 101(4):8297–8310

Renard P, Caers J (2008) Conditioning facies simulations with connectivity data in: Ortiz J, Emery X (eds.) Proceedings of the Eight International Geostatistics Congress volume 2 597–606 Gecamin ltd, Santiago

Saito T, Toriwaki J (1994) New algortihms for Euclidean distance transformation of an n-dimensional digital picture with applications. Pattern Recognit 27(11):1551–1565

Serra J (1988) Image analysis and mathematical morphology : theoretical advances. volume 2 Academic Press, London

Srivastava R, Frykman P, Jensen M (2004) Geostatistical simulation of fracture networks in: Leuangthong O, Deutsch C (eds.) Proceedings of the Seventh International Geostatistics Congress volume 1 295–304 Springer

Stoyan D, Kendall W, Mecke J (1995) Stochastic Geometry and its applications. John Wiley & sons, New York

Strebelle S (2002) Conditional simulation of complex geological structures using multiple-point statistics. Math Geol 34(1)

Viseur S (2004) Caractérisation de réservoirs turbiditiques : simulations stochastiques basées-objet de chenaux méandriformes Bull Soc Géol Fr 175(1):11–20

Xu W (1996) Conditional curvilinear stochastic simulation using pixel-based algorithms. Math Geol 28(7):937–949

Yin Y, Wu S, Zhang C, Li S, Yin T (2009) A reservoir skeleton-based multiple point geostatistics method. Sciences in China Series D: Earth Sciences 52:171–178

Yao T (1998) Conditional spectral simulation with phase identification. Math Geol 30(3):285–308

List of Figures

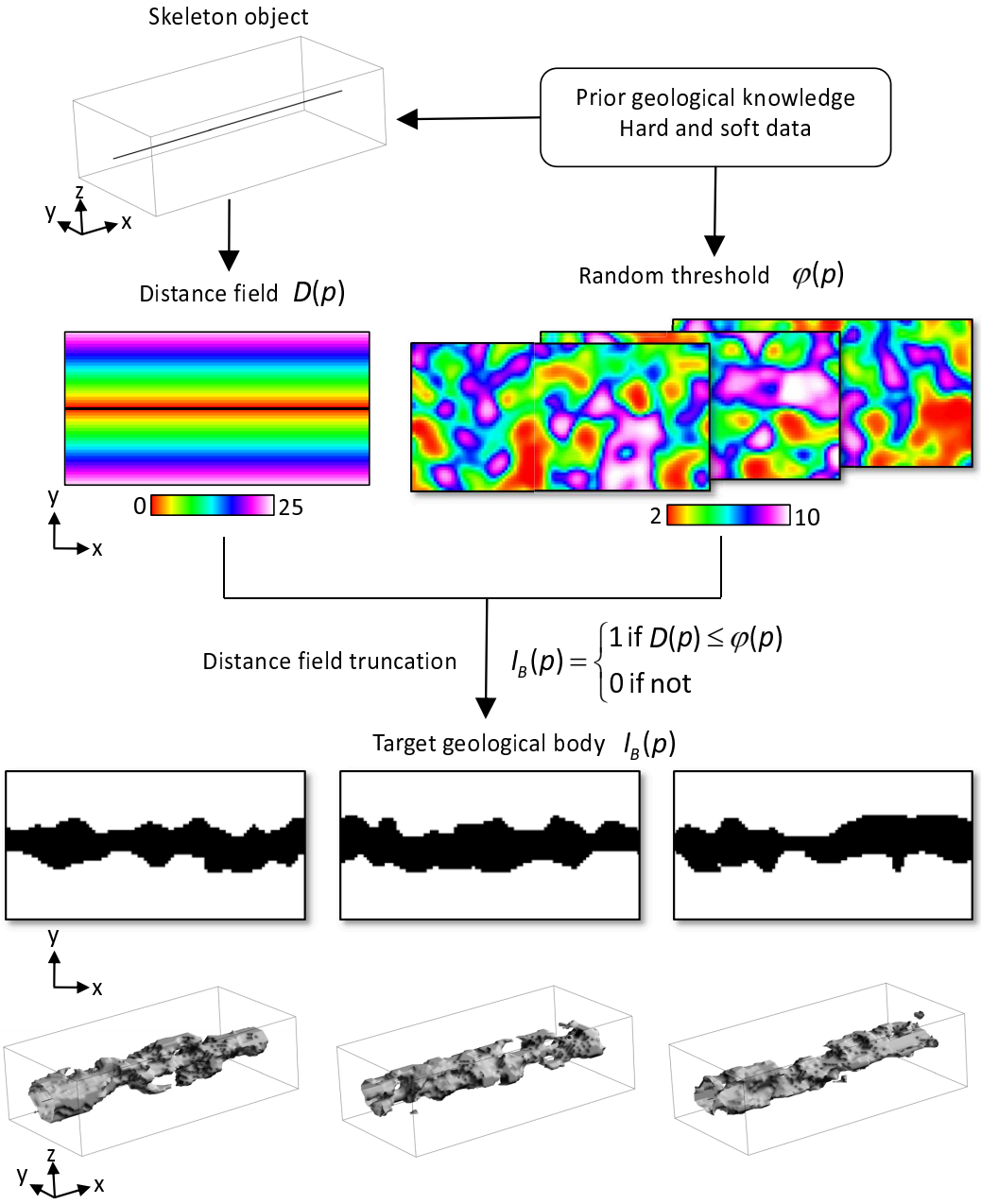

Figure 1: Workflow for object distance simulation. For one realization of a skeleton object (Section 2.2), its related distance field $D(p)$ (Section 2.3) is computed and truncated by a random threshold $\varphi(p)$ (Section 2.4) to obtain an indicator property of the target geological body $I_B(p)$.

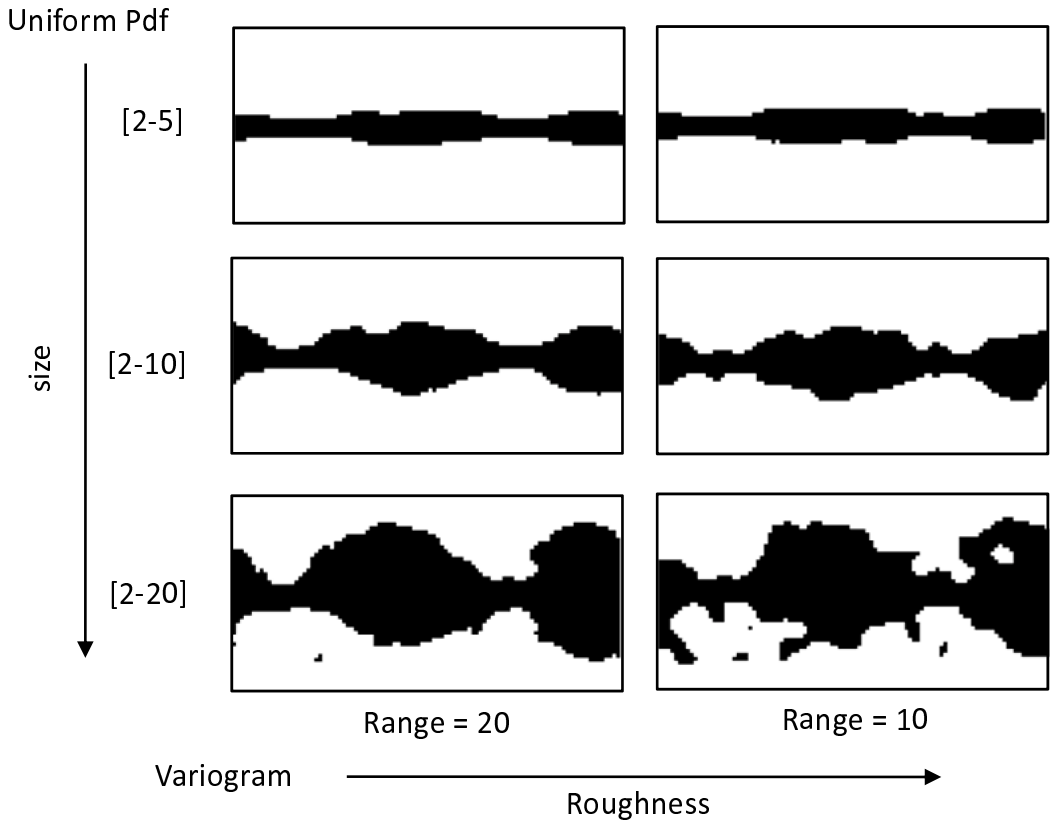

Figure 2: Influence of model parameters (same example as Figure 1)

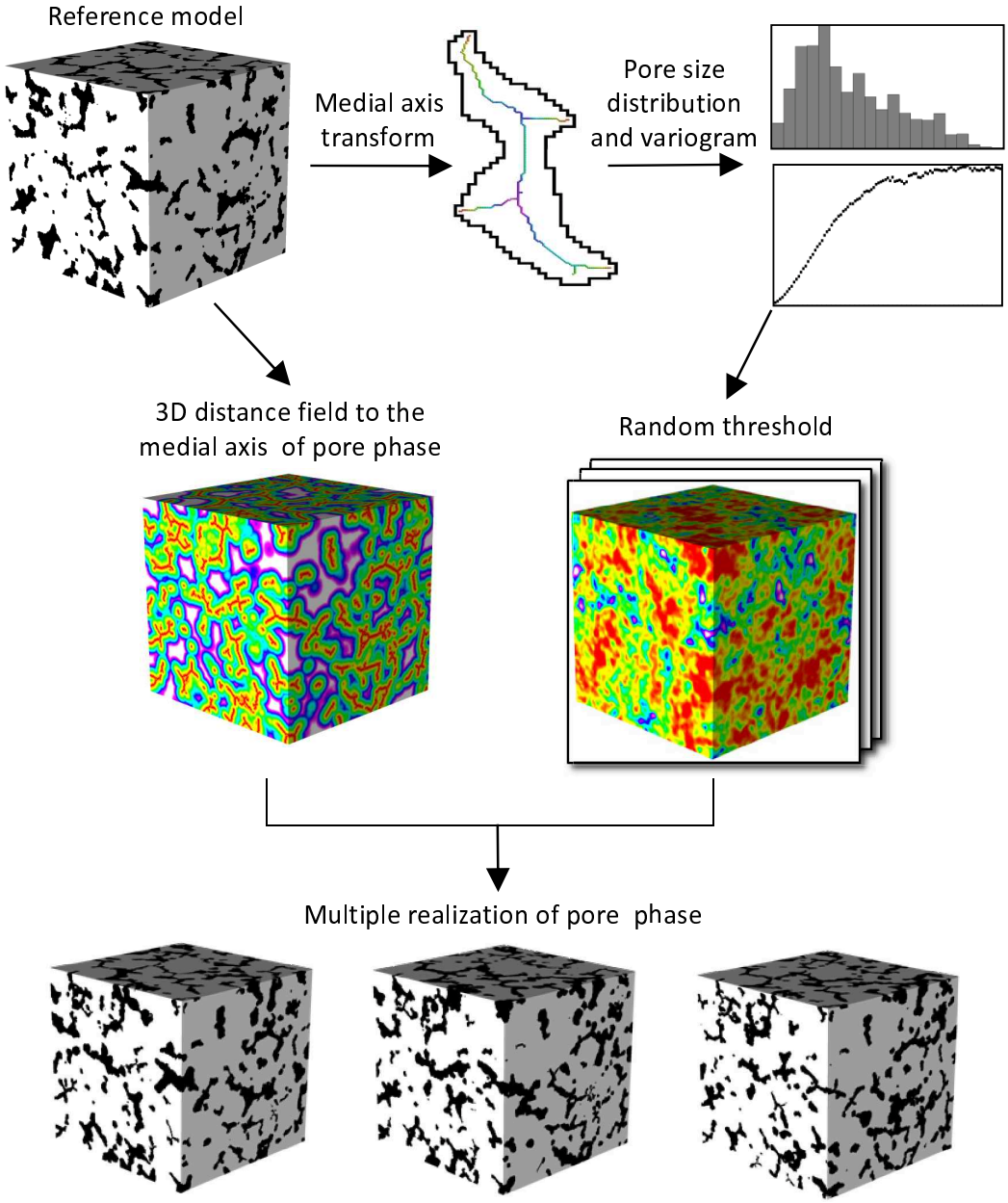

Figure 3: From a reference pore model, statistics about pore size distribution and spatial continuity is approximated based on the medial axis of the pores present in the training image. These statistics are then used to simulate random threshold fields. The final pore realizations are obtained by truncating the distance field to the medial axis of the reference pore model.

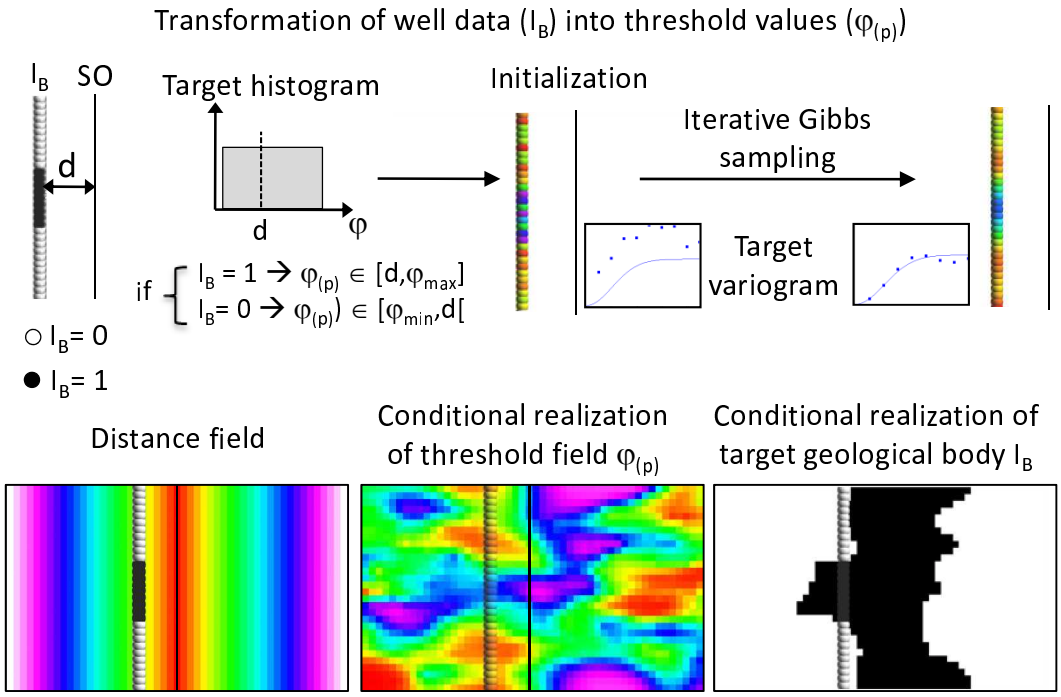

Figure 4: Workflow for data conditioning. The indicator property $I_{B(P)}$ is transformed into threshold values $\varphi_{\mathbf{p}}$ according to the target distribution and variogram model. These threshold values are then used to condition the SGS.

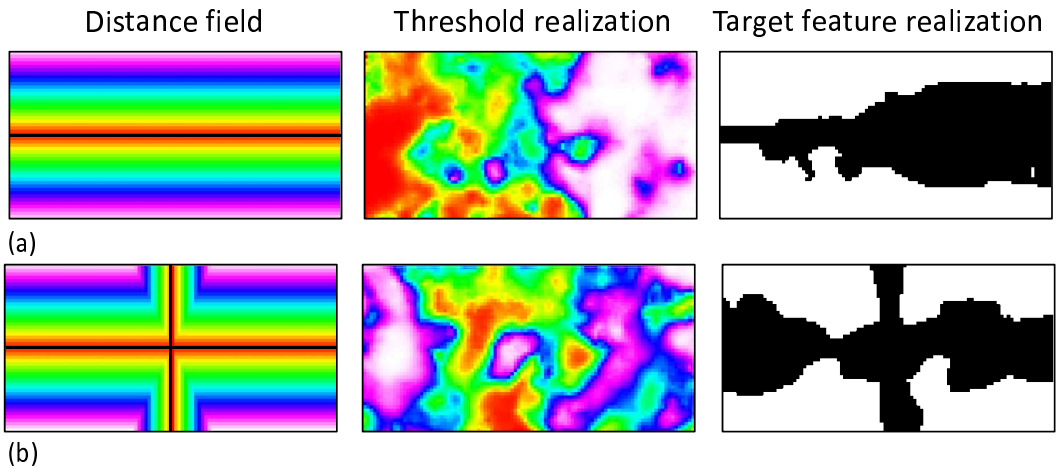

Figure 5: A, spatial trend in the object size has been introduced by specifying a locally variable mean, B, an anisotropic distance has been used to obtain objects with smaller (resp. greater) widths in the vertical direction (resp. horizontal direction).

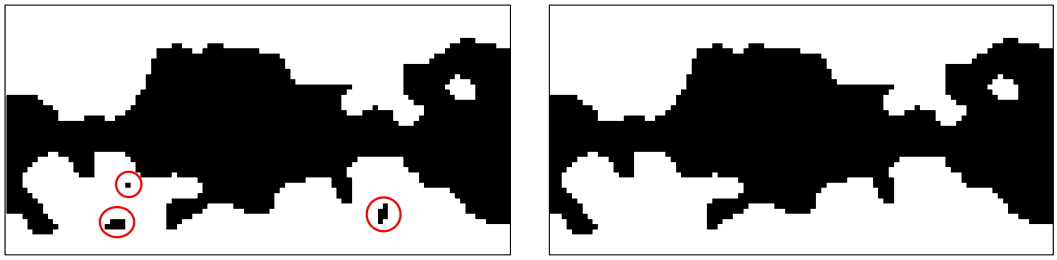

Figure 6: Post processing

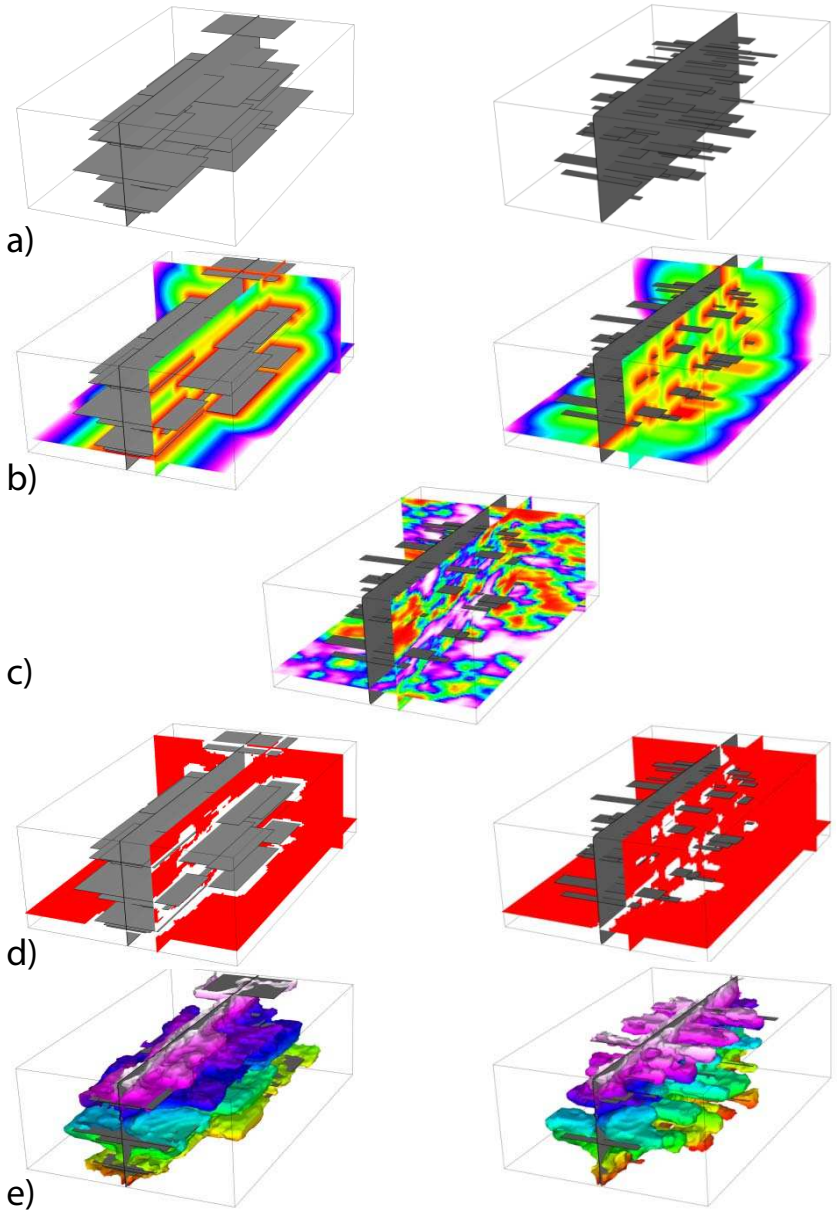

Figure 7: A, two different initial discrete object model, B, object-related distance field, C, random threshold, D, binary images of the dolomite bodies, and E, iso-surfaces of the dolomite bodies painted with depth values for better visualization

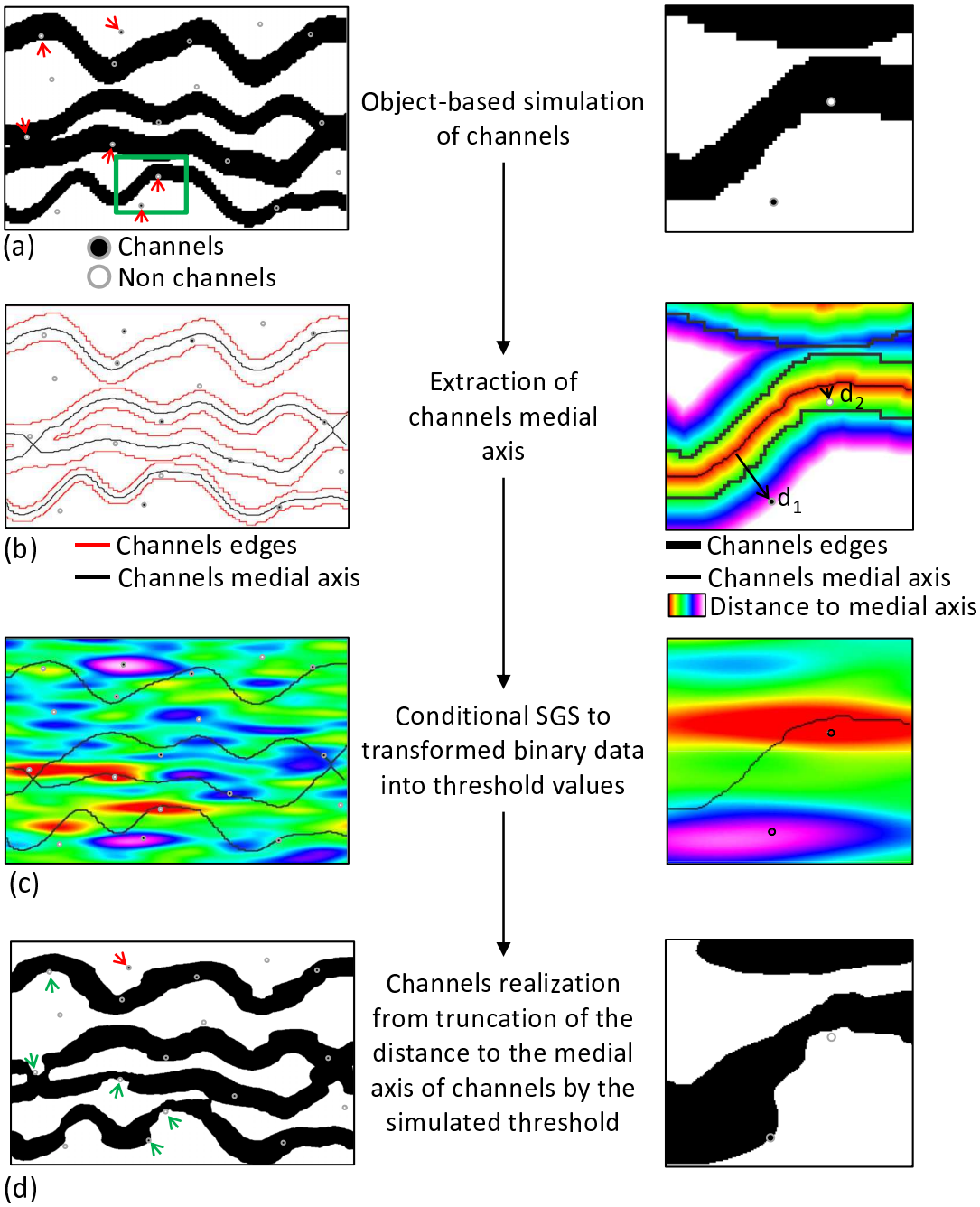

Figure 8: Improving data conditioning in channel simulation. Right column shows a detailed view. See text for details.